

Splenic response to protein corona of nanoparticles *in vivo*

Can Chen^a, Yueping Li^a, Dandan Zhou^a, Jiada Fan^a, Xuelan Hu^a, Ruru Zhang^a, Jianxian Ge^a, Xiaoyi Cao^a, Haodi Qi^a, Ning Wang^a, Lei Chen^a, Baoxing Huang^a, Jianfeng Zeng^{a,*}, Mingyuan Gao^{a,b,c,**}

^a Center for Molecular Imaging and Nuclear Medicine, State Key Laboratory of Radiation Medicine and Protection, School for Radiological and Interdisciplinary Sciences (RAD-X), Collaborative Innovation Center of Radiological Medicine of Jiangsu Higher Education Institutions, Soochow University, Suzhou 215123, China

^b School of Life Sciences, Soochow University, Suzhou 215123, China

^c The Second Affiliated Hospital of Soochow University, Suzhou 215123, China

ARTICLE INFO

Keywords:

Nanoparticles
Protein corona
Immune response
Spleen
Biological effect

ABSTRACT

The spleen is a meeting point between antigens transported by the blood stream and the immune apparatus responsible for mounting the host response. However, the interactions between nanomaterials and the spleen, significantly influenced by the protein corona formed on the surface of nanomaterials, are often overlooked. To address this issue, Fe₃O₄ nanoparticles with two distinct surface coatings, *i.e.*, diphosphonate-polyethylene glycol (DP-PEG), and diphosphonate- ϵ -aminocaproic acid (DP-EACA), were selected for a comprehensive investigation into the impacts of protein corona on the immune response within the spleen, attempting to gain a deeper understanding on how protein corona disturbs the immune response in the spleen to enrich the knowledge about the surface chemistry of nanoparticles. Additionally, carboxymethyl dextran (CM-DEX)-modified Fe₃O₄ nanoparticles, a generic form of the clinically used nanodrug Ferumoxytol, were chosen as a reference. The protein adsorption and its impacts on immune cells, gene expression, and metabolites in the spleen were investigated over a 28-day period. Our findings indicated that the opsonins carried by Fe₃O₄ nanoparticles were strongly correlated with immune response and metabolic disturbances in the spleen. However, DP-PEG coating exhibited remarkable resistance against protein adsorption and minimized spleen perturbation, highlighting its outstanding potential for clinical applications. All these findings are believed very valuable for developing clinically translatable drugs based on nanomaterials.

Introduction

Understanding the interactions between nanomaterials and the biological systems, as well as the consequent biological responses, is crucial for the biomedical applications of functional nanoparticles that have received intensive investigations over the past two decades [1]. Upon systemic administration, the majority of nanomaterials are typically taken up by the reticuloendothelial system (RES) and subsequently retained for prolonged periods mainly in the liver and spleen [2]. Although the interactions of nanomaterials with the liver have been extensively studied, the interactions with the spleen remain limited, primarily attributed to the comparatively lower accumulation of nanomaterials in the latter [3]. However, it's crucial to note that the spleen

also serves as a significant venue for nanomaterials to interact biological systems. One of the primary functions of the spleen is to remove foreign nanomaterials from the blood. Nanomaterials enter the spleen through the splenic artery, where they are captured by macrophages and other immune cells [4]. Subsequently, these nanomaterials undergo gradual degradation. Together with the degradation products, they can be transported out of the spleen to participate in systemic metabolism [5]. For example, Chen et al. found that MoS₂ nanomaterials of 3.3 nm × 1.9 nm in the spleen were degraded into MoO₄²⁻ which was transported through the splenic vein to the hepatic portal vein and ultimately participated in the synthesis process of molybdenum enzymes in hepatocytes [4]. Additionally, the spleen serves as a meeting point between antigens transported by the bloodstream and the immune system for

* Corresponding author.

** Corresponding author at: Center for Molecular Imaging and Nuclear Medicine, State Key Laboratory of Radiation Medicine and Protection, School for Radiological and Interdisciplinary Sciences (RAD-X), Collaborative Innovation Center of Radiological Medicine of Jiangsu Higher Education Institutions, Soochow University, Suzhou 215123, China.

E-mail addresses: jfzeng@suda.edu.cn (J. Zeng), gaomy@suda.edu.cn (M. Gao).

<https://doi.org/10.1016/j.nantod.2025.102676>

Received 9 November 2024; Received in revised form 1 February 2025; Accepted 17 February 2025

Available online 1 March 2025

1748-0132/© 2025 Elsevier Ltd. All rights reserved, including those for text and data mining, AI training, and similar technologies.

initiating the host response [6]. As the largest secondary lymphoid organ in the body, the spleen possesses strong immunologic functions. Thus, the retention of nanomaterials in the spleen may stimulate strong immune responses [6,7]. On the one hand, the activation of the immune system may lead to adverse immune stimulation and potential associated side effects, including inflammation, hypersensitivity, and allergic reactions [8–11]. On the other hand, immune stimulation can also be potentially utilized in oncological applications, for instance, in constructing nanovaccines to stimulate the immune system to produce effective anti-tumor immune responses [12,13]. Therefore, exploring the interactions between nanomaterials and the spleen, especially the subsequent immunological effects, is significant for designing biomedical nanomaterials with reduced immunotoxicity.

Numerous studies have shown that the surface adhesion of proteins endows the underlying nanomaterials with new biological characteristics, which may significantly influence their interactions with the spleen. Generally, once nanomaterials enter the bloodstream, abundant protein molecules quickly bind to their surface, forming a “protein corona” [14, 15]. At the interface that controls the interactions between nanomaterials and biological systems, the protein corona plays a pivotal role in inducing noteworthy changes in their biological behavior [16,17]. Previous studies have demonstrated that protein corona not only governs the uptake behavior of nanomaterials by the spleen, but also affects the immune response induced by nanomaterials within the spleen [4, 18]. For instance, the aforementioned MoS₂ nanomaterials were found to mainly locate in the red pulp region of spleen after entry and the coronal apolipoprotein E (APOE) increased the uptake of these nanomaterials by splenic red pulp macrophages [4]. Similarly, Khang et al. found that carbon nanotubes could increase reactive oxygen species (ROS) levels in the spleen and trigger the activation of pro-inflammatory cytokines, as well as subsequent innate and adaptive immune responses [18]. The immune stimulation was primarily attributed to the highly unfolded protein corona structure pre-coated on their surface. In this aspect, the protein corona emerges as a pivotal factor for understanding the potential toxicity of nanomaterials through the interactions between nanomaterials and the spleen.

Among various kinds of nanoparticles, Fe₃O₄ nanoparticles have gained significant attention in the biomedical field due to their unique physical and chemical properties, as well as their excellent biocompatibility [19,20]. Several types of Fe₃O₄ nanoparticles synthesized *via* the coprecipitation method got approved by the Food and Drug Administration (FDA) back to 1996. However, Fe₃O₄ nanoparticles for magnetic resonance imaging (MRI) applications didn't present good enough clinical performance as expected [21,22]. Currently, only one type of Fe₃O₄ nanoparticles-based nanodrug, Ferumoxytol, is still in clinical use as an iron supplement [21]. Notably, the FDA issued a warning in 2015 about the potential life-threatening allergic reactions caused by intravenous injections of Ferumoxytol [23]. This phenomenon underscores the necessity to pay special attention to the immune effects produced by nanoparticles in the body. With advancements in synthesis and surface modification technologies, the performance of Fe₃O₄ nanoparticles has been greatly improved [24–26]. In particular, ultrasmall Fe₃O₄ nanoparticles, showing excellent T₁ contrast enhancement effect, is becoming a potential candidate as the next generation clinical MRI contrast agents [27,28]. Although the effectiveness of ultrasmall Fe₃O₄ nanoparticles is well-recognized, the lack of comprehensive understanding of their interactions with the immune system poses potential risks to their clinical translation.

In this study, the biological effects of three types of Fe₃O₄ nanoparticles on the spleen, *i.e.*, Fe₃O₄@PEG, Fe₃O₄@EACA, and Fe₃O₄@DEX, were systematically investigated with a specific focus on the role of the protein corona, aiming to improve our understanding on the interactions between Fe₃O₄ nanoparticles and biological systems. Comprehensive quantitative and qualitative analyses of the protein corona formed on these nanoparticles were conducted first. Subsequently, their effects on immune cells, gene expression, and metabolites

in the spleen of mice at different time points over 28 d were investigated to elucidate the local perturbations caused by Fe₃O₄ nanoparticles *in vivo*. Additionally, a series of safety evaluation experiments were performed to assess the biocompatibility of Fe₃O₄ nanoparticles. The exploration of such nanomaterials-spleen interactions is expected to enrich our knowledge on the *in vivo* fate and mechanisms for improving the biosafety of nanomedicine.

Results

Synthesis and characterization of Fe₃O₄ nanoparticles

Ultrasmall Fe₃O₄ nanoparticles with core diameters smaller than 5 nm are expected to become the next generation of MRI contrast agents due to their superior MRI properties and excellent biocompatibility [27, 29,30]. Therefore, hydrophobic Fe₃O₄ nanoparticles of 3.8 ± 0.7 nm were synthesized herein using a slightly modified thermal decomposition method previously reported (Fig. S4) and then transferred into water to become MR contrast agents [24]. Given that the binding affinity of diphosphonate (DP) groups with Fe³⁺ is higher than that of the anchoring group of the initial hydrophobic ligands, diphosphonate-polyethylene glycol (DP-PEG, Mw = 2000) and diphosphonate- ϵ -aminocaproic acid (DP-EACA) were designed, synthesized and employed to endow Fe₃O₄ nanoparticles with water-solubility through ligand exchange [31,32]. The structures of DP-PEG and DP-EACA are displayed in Fig. 1a. PEG, known for its excellent biocompatibility, is widely used as a surface ligand in biomedical applications and is renowned for its antifouling properties [33,34]. DP-EACA, a small molecular surface ligand with abundant negative charges, is expected to adsorb fewer proteins than positively charged ligand modified nanoparticles. In addition, carboxymethyl dextran (CM-DEX, Mw = 40k, Fig. 1a) coated Fe₃O₄ nanoparticles (denoted as Fe₃O₄@DEX) were chosen as a reference, mirroring Ferumoxytol, an FDA-approved Fe₃O₄ nanoparticle for treating iron deficiency [35]. As shown in Fig. 1b, c, the representative transmission electron microscope (TEM) images and the corresponding particle size distribution profiles indicate that nearly monodispersed Fe₃O₄ nanoparticles coated with PEG, denoted as Fe₃O₄@PEG, and DP-EACA modified Fe₃O₄ nanoparticles, denoted as Fe₃O₄@EACA, are successfully obtained. There is no significant change in particle size or size distribution profile after the surface modification with the hydrophilic ligands. In contrast, Fe₃O₄@DEX, obtained through the co-precipitation method, exhibits highly similar morphologies as Ferumoxytol, characterized by irregular morphologies and inhomogeneous particle sizes, as seen in Fig. 1d.

Dynamic light scattering (DLS) was carried out to further evaluate the hydrodynamic properties of the as-prepared water-soluble Fe₃O₄ nanoparticles. The results in Fig. 1e indicate that Fe₃O₄@PEG, Fe₃O₄@EACA, and Fe₃O₄@DEX exhibit single scattering peaks locating at 14.7 ± 0.5 nm, 6.9 ± 0.3 nm, and 43.0 ± 1.2 nm, respectively. The significant variation in the hydrodynamic size of these hydrophilic Fe₃O₄ nanoparticles can be attributed to the differences in both molecular weight of surface ligands and particle core size. To evaluate the colloidal stability, the as-prepared hydrophilic Fe₃O₄ nanoparticles were incubated in HEPES buffer for up to 3 d, with their hydrodynamic sizes monitored using DLS. As depicted in Fig. S5, the variations in hydrodynamic size were negligible, indicating excellent colloidal stability of the obtained Fe₃O₄ nanoparticles. Zeta potential measurements were conducted to characterize these three kinds of Fe₃O₄ nanoparticles. As indicated in Fig. 1f, Fe₃O₄@PEG exhibits a weak negative surface charge of -10.4 ± 0.6 mV, originating from the spare -P-O⁻ moieties of the DP anchoring groups after coordination with Fe³⁺ ions [36]. Fe₃O₄@EACA shows a stronger negative surface charge of -21.8 ± 3.8 mV, due to carboxylate groups apart from -P-O⁻ residues. Fe₃O₄@DEX displays the strongest negative surface charge down to -25.6 ± 2.1 mV, owing to the presence of a large number of carboxylate groups in the coating layer. The negative surface charges of all three types of nanoparticles are

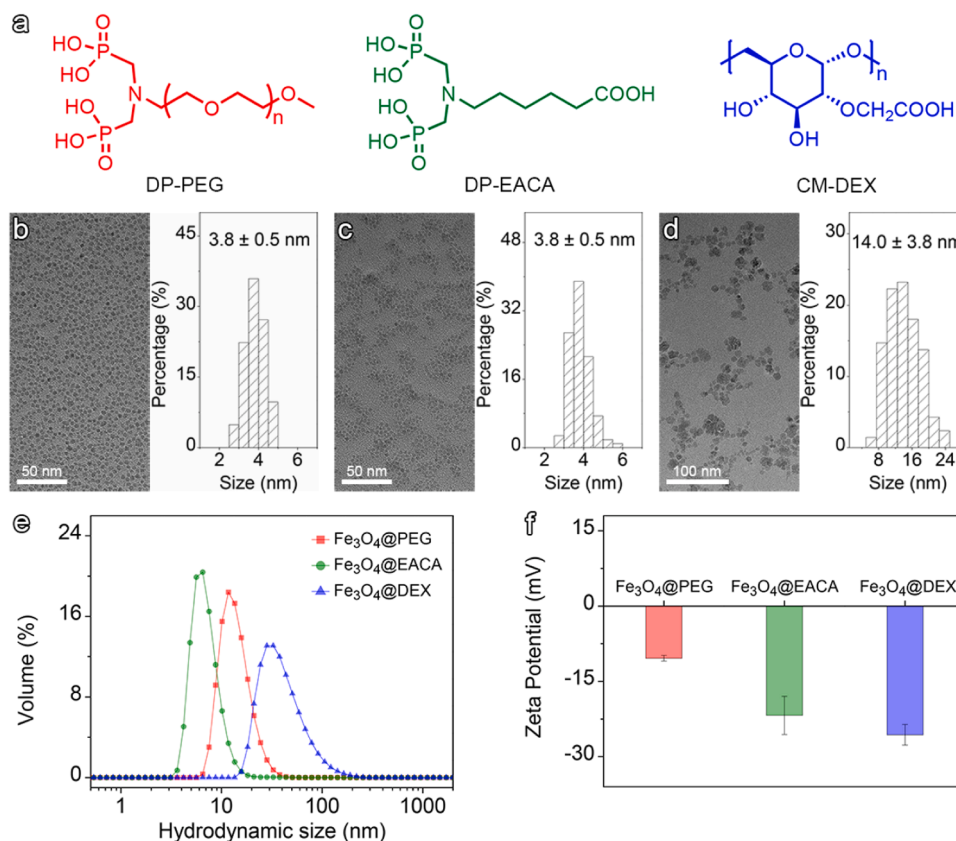


Fig. 1. Characterization of hydrophilic Fe_3O_4 nanoparticles. (a) Chemical structures of surface ligands of Fe_3O_4 nanoparticles. TEM images and corresponding particle size distributions of (b) Fe_3O_4 @PEG, (c) Fe_3O_4 @EACA, and (d) Fe_3O_4 @DEX. (e) Hydrodynamic size distribution and (f) zeta potential of three types of Fe_3O_4 nanoparticles.

generally favorable for reducing their interactions with plasma proteins [14,37].

Analysis of protein corona on Fe_3O_4 nanoparticles

According to previous literatures, it has been learnt that the surfaces of nanomaterials are rapidly coated with a protein corona upon contact with blood, which significantly redefines the biological properties of the nanomaterials [14,38,39]. To elucidate the nature of the protein corona, Fe_3O_4 @PEG, Fe_3O_4 @EACA, and Fe_3O_4 @DEX were incubated in mouse plasma, respectively, followed by the collection and identification of corona proteins on the particle surfaces, as illustrated in Fig. 2a. By using the clinical injection dosage of MRI contrast agents (0.1 mmol Fe/kg body weight), the *in vivo* concentration of Fe_3O_4 nanoparticles in mice was estimated to be around 100 μg Fe/mL. To better match the *in vivo* conditions, the incubation concentration of Fe_3O_4 nanoparticles in mouse plasma *in vitro* was also set at 100 μg Fe/mL. The total amount of proteins adsorbed on the surface of nanoparticles was quantified using the Bicinchoninic Acid (BCA) assay. As shown in Fig. 2b, the protein adsorption capacity follows an order of Fe_3O_4 @EACA > Fe_3O_4 @DEX > Fe_3O_4 @PEG.

In addition to protein adsorption capacity, the components of the protein corona were also analyzed. The corona proteins were separated using one-dimensional sodium dodecyl sulfate-polyacrylamide gel electrophoresis (SDS-PAGE) and then analyzed through Coomassie Brilliant Blue staining. As shown in Fig. 2c, the components of the protein corona differ markedly from those in mouse plasma. The high-abundance mouse plasma proteins are mainly located around 75, 68, 50, and 25 kDa. In contrast, the corona proteins are primarily located around 75, 50, and 25 kDa, with albumin (ALB, 68 kDa), the main component of plasma proteins, being absent.

Since SDS-PAGE cannot provide detailed information on specific proteins, further liquid chromatography-mass spectrometry/mass spectrometry (LC-MS/MS) analysis were carried out, in combination with peptide fragmentation analysis, to accurately identify the protein components of the corona. The Venn diagrams displayed in Fig. 2d show the number of common and unique proteins in the protein corona of Fe_3O_4 nanoparticles. A total number of 631, 717, and 340 types of proteins are found adsorbed on Fe_3O_4 @PEG, Fe_3O_4 @EACA, and Fe_3O_4 @DEX, respectively. Among them, 176 types of proteins are in common. The number of common types of adsorbed proteins is insufficient enough to fully reflect the complexity of the protein corona. To better understand the effects of surface ligands on the protein corona, the relative protein abundance of each identified protein was calculated.

As the fingerprints, the protein corona may markedly affect the recognition of nanoparticles by biological systems including different type of cells and tissues, because different types of proteins perform distinct roles in the body. In order to better understand the protein corona, the protein components were categorized into four types according to their physiological functions, such as immunoglobulins, apolipoproteins, coagulations, and complements. As shown in Fig. 3a, immunoglobulins constitute the majority of the protein corona, accounting for 59.4 % for Fe_3O_4 @PEG, 37.9 % for Fe_3O_4 @EACA, and 47.1 % for Fe_3O_4 @DEX. Immunoglobulins are primarily involved in immune response, responsible for recognizing and binding antigens [40, 41]. According to more detailed data on protein compositions and respective quantities presented in Fig. 3b, it can be found that immunoglobulin heavy constant mu (IGHM) exhibits the highest contents in all three types of Fe_3O_4 nanoparticles, which is consistent with the of SDS-PAGE results showing prominent protein bands at 50 kDa for all three samples (Fig. 2c). Apolipoproteins are the protein components of plasma lipoproteins that bind and transport blood lipids to various

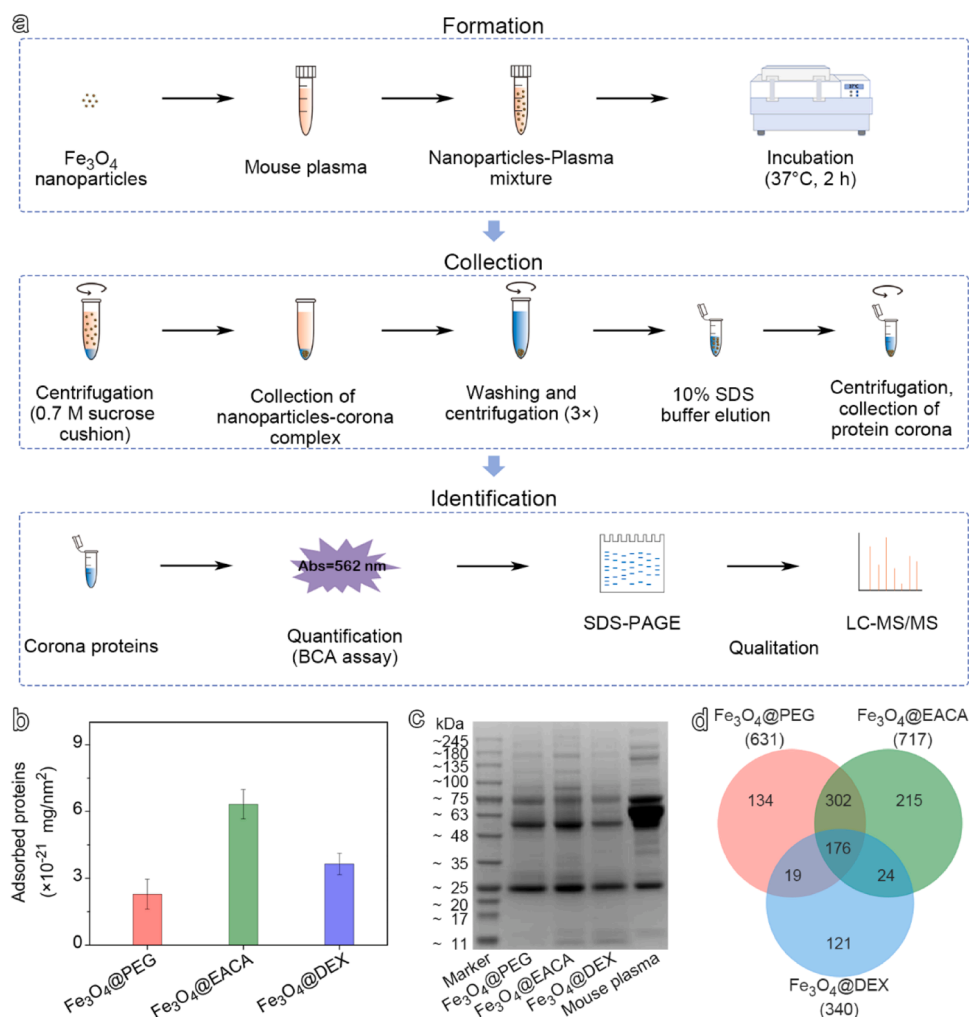


Fig. 2. Proteomic study of protein corona on Fe_3O_4 nanoparticles. (a) Schematic representation of the separation and analysis process for protein corona on Fe_3O_4 nanoparticles. (b) Quantitative analysis of protein corona per unit area of Fe_3O_4 nanoparticles using BCA assay. (c) SDS-PAGE images showing proteins detached from Fe_3O_4 nanoparticles after incubation with mouse plasma. (d) Venn diagrams depicting common proteins and unique proteins identified in the protein corona of each Fe_3O_4 nanoparticles type.

tissues in the body for metabolism and utilization [40]. As shown in Fig. 3b, apolipoprotein A-I (APOA1) dominates the apolipoproteins in the corona of Fe_3O_4 @PEG and Fe_3O_4 @DEX. With respect to Fe_3O_4 @EACA, APOE content is the highest followed by APOA1. In addition, APOE also takes at least the third place with respect to the adsorption quantity for Fe_3O_4 @PEG and Fe_3O_4 @DEX. Coagulation proteins are involved in the blood coagulation process [40]. Platelet factor 4 (PF4) dominates coagulation proteins in the coronas of Fe_3O_4 nanoparticles, except for Fe_3O_4 @EACA. In the latter case, thrombospondin-1 (THBS1) becomes dominant. Coagulation proteins are also a part of opsonins and are associated with complement activation and immune response. Studies have shown that the complex of PF4 and heparin contributes to C9 activation through the lectin pathway [42]. Complement proteins are present in serum and tissue fluid, and upon activation, they exhibit enzymatic activity that can mediate immune and inflammatory responses [40]. Complement C1q subcomponent subunit B (C1QB) is abundantly present in all protein coronas (Fig. 3b). Complement 3 (C3) is another highly abundant protein found in the protein corona of Fe_3O_4 @EACA and Fe_3O_4 @DEX. It plays a central role in the activation of the complement system.[43] The overall abundance of immunoglobulins, complements, and coagulations on Fe_3O_4 @EACA and Fe_3O_4 @DEX is much higher than that on Fe_3O_4 @PEG, suggesting that these nanoparticles may trigger stronger immune disturbances *in vivo*.

Molecular weight and isoelectric point (pI) are two other crucial characteristics of a given protein. According to the analytic results in Fig. S6a, proteins with a molecular weight less than 60 kDa accounted for 73.5–85.0 % of the total proteins, consistent with the observed results in SDS-PAGE image (Fig. 2c). According to pI analysis, as shown in Fig. S6b, most corona proteins displayed a pI less than 7.4, which may be attributed to the fact that a significant proportion of plasma proteins are negatively charged under physiological conditions [44].

The top 20 most abundant proteins adsorbed on the surface of Fe_3O_4 nanoparticles were identified and compared with the top 20 mouse plasma proteins in Supplementary Table 1. The highest abundance proteins were significantly different, with IGHM for protein coronas and ALB for mouse plasma. Only five common proteins were found in common between those in mouse plasma and the protein corona, *i.e.*, IGHM, immunoglobulin kappa constant (IGKC), pregnancy zone protein (PZP), ALB, and immunoglobulin heavy constant gamma 2B (IGHG2B). This indicates that surface chemistry significantly influences the composition of protein coronas, remarkably increasing their complexity. Next, the contents of high-abundance proteins in protein corona with a relative abundance above 2 % were analyzed and compared with those in mouse plasma (Fig. S7). Several high-abundance proteins with relative abundances higher than 5 %, such as IGHM, IGHA, PF4, APOE, and MBL1, were found present on the surface of at least one type of Fe_3O_4 nanoparticles, were not highly abundant in mouse plasma (< 1 %).

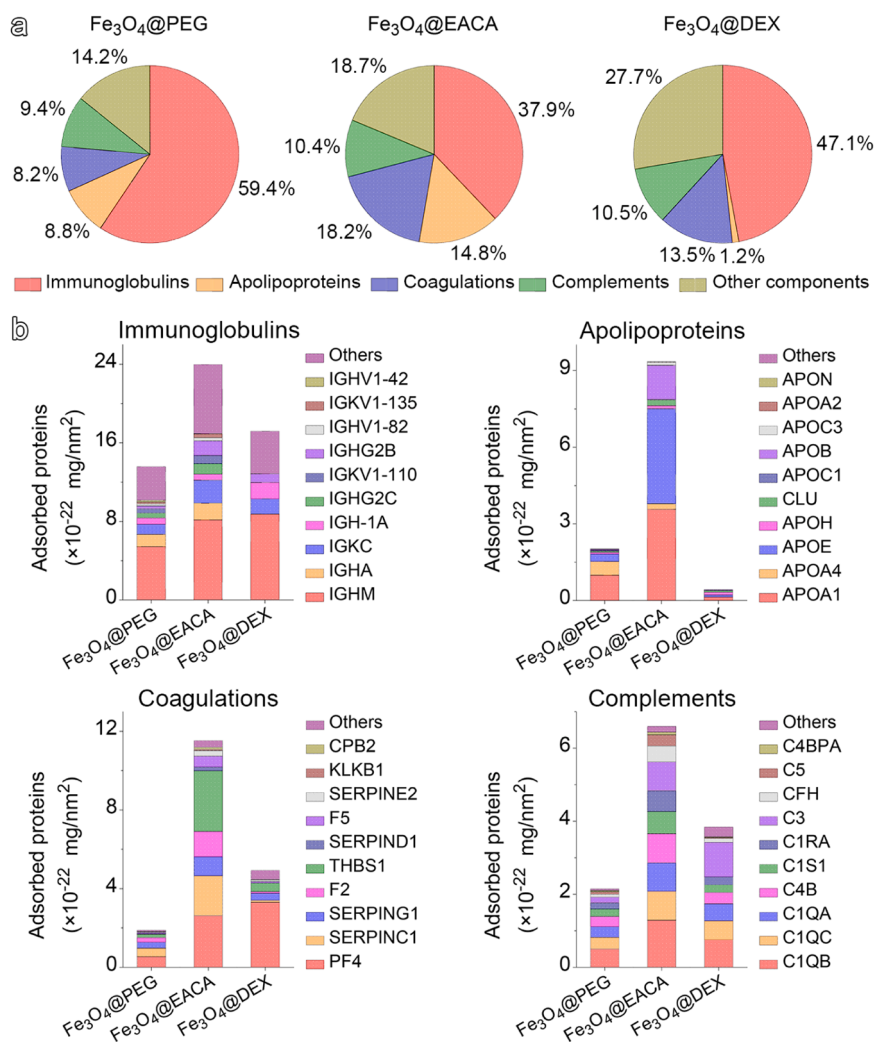


Fig. 3. Bioinformatic classification of protein corona components. (a) Categories of corona proteins based on their functions in biological processes. (b) Quantitative analysis of the protein corona components identified on the surface of Fe₃O₄ nanoparticles.

Although ALB is the most abundant protein in mouse plasma, accounting for about half of the total plasma protein quantity, its levels in the three protein coronas were lower than expected ($< 5\%$). Most high-abundance proteins in the coronas are not highly abundant in mouse plasma, suggesting that these low-abundance proteins have a stronger affinity to Fe₃O₄ nanoparticles. The formation of the protein corona is actually a dynamic and competitive process. The high-abundance proteins do enjoy a much higher probability to interact with the nanoparticles once they are introduced into biological fluids. But these high-abundance proteins are gradually replaced by proteins with higher affinity for nanoparticles over time, forming a stable “hard corona” [44]. Therefore, enrichment factors of different Fe₃O₄ nanoparticles for various proteins in mouse plasma were calculated to compare the affinity of different corona proteins to Fe₃O₄ nanoparticles. As shown in Fig. S8, IGHM, PF4, and C1QB exhibited significant enrichment effects in all three types of Fe₃O₄ nanoparticles. Additionally, APOE, VTN, and THBS1 were also highly enriched in Fe₃O₄@EACA. On the surface of Fe₃O₄@DEX, MBL1, Ig gamma-2A chain C region secreted form, and HBB-B1 were also found highly enriched. The highly abundant protein MBL1, playing an important role in innate immune responses by mediating the activation of the lectin complement pathway [45], is particularly notable. Taken together, the above results indicate a distinct, surface chemistry-dependent nanomaterials-proteins binding pattern, in which Fe₃O₄@EACA and Fe₃O₄@DEX not only exhibit higher levels of proteins adsorption than Fe₃O₄@PEG, but also show a stronger protein

enrichment ability that is associated with the immune responses.

Biodistribution of Fe₃O₄ nanoparticles

For gaining comprehensive information on the biological distribution of three types of Fe₃O₄ nanoparticles, inductively coupled plasma-optical emission spectrometer (ICP-OES) was utilized to quantify Fe elements in mouse tissues after a single tail vein injection with a dose of 0.1 mmol Fe/kg body weight. Two time points (short and long; 1 d and 28 d, respectively) were adopted for assessing the possible toxic responses of all three types of Fe₃O₄ nanoparticles (Fig. 4a). Due to the high background level of Fe in tissues, a significant amount of Fe element was detected in the saline group. In contrast, the Fe₃O₄ nanoparticles showed increased Fe levels in the liver and spleen 1 d post-injection, while Fe levels in other organs, including the heart, lung, kidney, and brain, weren't significantly increased, as displayed in Fig. S9, indicating that the majority of the three types of Fe₃O₄ nanoparticles are primarily captured and accumulated in the RES-related organs. Furthermore, the Fe levels of the liver and spleen were noticeably decreased 28 d post-injection, approaching the levels of the negative control, suggesting a reduction of Fe accumulation over time. This result demonstrates that at the dosage level used in this study, Fe₃O₄ nanoparticles do not lead to long-term accumulation in the body, nor do they significantly alter the overall iron levels.

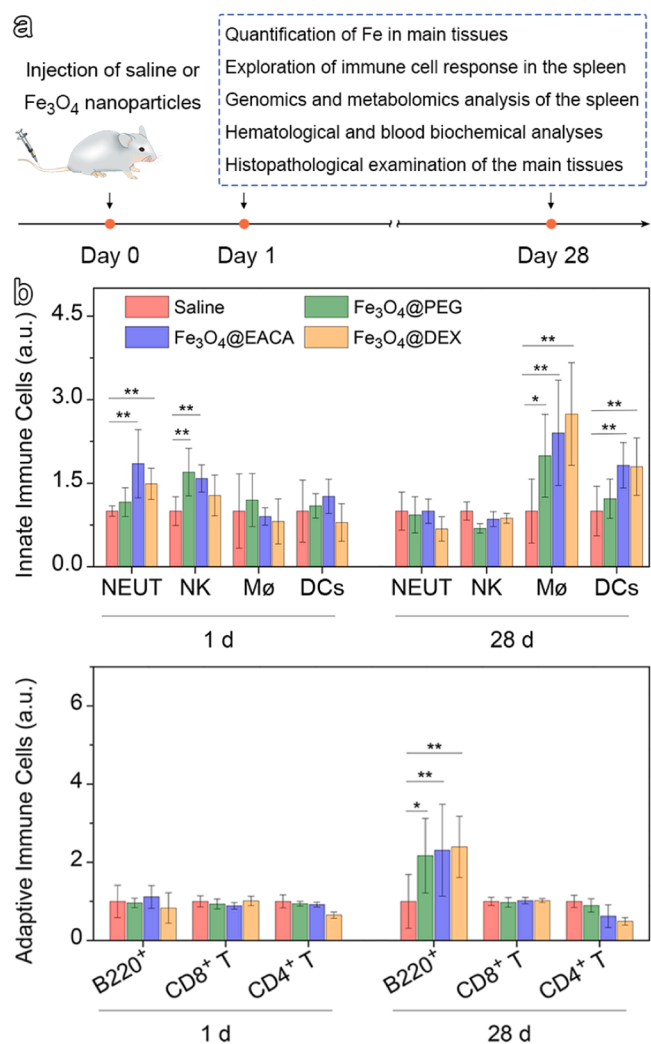


Fig. 4. Innate and adaptive immune cell responses of mice. (a) Schematic illustration of *in vivo* experiments involving intravenous injection of saline and Fe₃O₄ nanoparticles into female BALB/c mice. (b) FACS analysis of isolated innate immune cells (NEUT, NK, M ϕ , and DCs) and adaptive immune cells (B cells, and T cells (CD8⁺ and CD4⁺)) from the spleen after intravenous injection of saline and Fe₃O₄ nanoparticles. NEUT: Neutrophils; NK: Natural killer; M ϕ : Macrophages; DCs: Dendritic cells.

Innate and adaptive immune cell responses

Given the presence of various innate and adaptive immune cells in the spleen, their interactions with Fe₃O₄ nanoparticles are unavoidable. It has been reported that foreign substances may induce immune responses associated with the proliferation of immune cells [7,18]. To explore whether Fe₃O₄ nanoparticles can affect the proliferation of immune cells in the spleen, the immune cells populations were examined. One day after the intravenous injection of the particles, significant effects on innate immune cells were observed. Specifically, as shown in Fig. 4b, neutrophils in the Fe₃O₄@EACA and Fe₃O₄@DEX groups, as well as natural killer (NK) cells in the Fe₃O₄@PEG and Fe₃O₄@EACA groups, show improved proliferation. However, no changes in macrophages, dendritic cells (DCs), or adaptive immune cells (B cells, CD4⁺ T cells, and CD8⁺ T cells) are observed in any Fe₃O₄ nanoparticles groups. These results demonstrate that one day after injection of Fe₃O₄ nanoparticles, the innate immune responses in the spleen are triggered, but not sufficient to elicit adaptive immune responses. In difference, 28 d after the injection of the nanoparticles, the populations of neutrophils and NK cells have returned to baseline levels. But the levels of

macrophages and B cells are significantly increased in all three nanoparticle groups, if compared with those of the saline group. In addition, the frequency of DCs is also affected by Fe₃O₄@EACA and Fe₃O₄@DEX.

Alterations of gene expression in mouse spleen

To further investigate the short-term effects following exposure to Fe₃O₄ nanoparticles, differentially expressed genes (DEGs) in the spleens from three pairwise groups (Fe₃O₄@PEG vs. saline, Fe₃O₄@EACA vs. saline, Fe₃O₄@DEX vs. saline) were identified through LC-MS/MS (Fig. S10). As shown in Fig. 5a, a total of 41 genes (22 up-regulated and 19 down-regulated) are identified as DEGs one day after exposure to Fe₃O₄@PEG. Compared with the control, 124 DEGs (80 up-regulated and 44 down-regulated) are found in Fe₃O₄@EACA group. With respect to Fe₃O₄@DEX group, 287 DEGs are detected, with 156 DEGs showing up-regulated expression and 131 DEGs showing down-regulated expression. Notably, Fe₃O₄@PEG exhibits weaker impacts on gene expression in the spleen than Fe₃O₄@EACA and Fe₃O₄@DEX.

These DEGs were further annotated using Gene Ontology (GO) databases to reveal their specific functions that were primarily categorized into cellular components, biological processes, and molecular functions. The top 20 GO pathways were provided, with an emphasis on those pathways related to immune responses. GO enrichment results in Fig. 5b reveal that DEGs in the Fe₃O₄@PEG group are primarily enriched in metabolic processes, *i.e.*, melanin biosynthetic process, one-carbon metabolic process, and positive regulation of microtubule nucleation, with a small amount enriched in immune response pathways, such as defense response to virus, *etc.* In contrast, significant numbers of DEGs associated with immune responses are observed in both the Fe₃O₄@EACA group and Fe₃O₄@DEX group, which becomes particularly evident in the top 6 GO pathways, *i.e.*, defense response to virus, response to virus, innate immune response, immune system process, response to bacterium, regulation of viral entry into host cell, and negative regulation of viral genome replication, as shown in Fig. 5c, d. Moreover, there are a large number of DEGs related to innate immune responses in the Fe₃O₄@EACA and Fe₃O₄@DEX groups, indicating that these nanoparticles trigger stronger immune effects. Additionally, a significant number of DEGs are found related to lipid metabolism in the Fe₃O₄@EACA group, suggesting that lipid metabolism in the spleen can also be affected.

Enrichment analysis was also performed using Kyoto Encyclopedia of Genes and Genomes (KEGG) database to assess the biological significance of these DEGs. Only the top 20 most abundant KEGG pathways were displayed in Fig. S11. It was observed that the DEGs in the Fe₃O₄@PEG group were mostly enriched in the metabolism-related pathways, such as nitrogen metabolism and tyrosine metabolism (Fig. S11a). Meanwhile, Fig. S11b, c showed that the primarily relevant pathways of DEGs were influenza A and measles in the Fe₃O₄@EACA group, as well as complement and coagulation cascades, and IL-17 signaling pathways in the Fe₃O₄@DEX group, all of which are associated with immune responses. From the above results, it can easily be concluded that Fe₃O₄@EACA and Fe₃O₄@DEX trigger stronger immune responses in mouse spleens than Fe₃O₄@PEG over short-term exposure, *e.g.*, 1 d.

In addition, to assess the long-term effects on the spleen, DEGs between the control group and three Fe₃O₄ nanoparticles groups were also screened 28 d postinjection (Fig. S12). As shown in Fig. 5e, significant changes are revealed. Compared with the saline group, the Fe₃O₄@PEG group presents 122 upregulated and 819 downregulated DEGs, the Fe₃O₄@EACA group shows 1047 upregulated and 749 downregulated DEGs, and the Fe₃O₄@DEX group displays 183 upregulated and 685 downregulated DEGs. The numbers of DEGs in each group are significantly increased, in comparison to those recorded 1 d postinjection, indicating a significant and exacerbating impacts of Fe₃O₄ nanoparticles on the spleen over long-term, *e.g.*, 28 d. GO enrichment analysis of these DEGs, as provided in Fig. 5f-h, show that cell-cell interactions (*e.g.*,

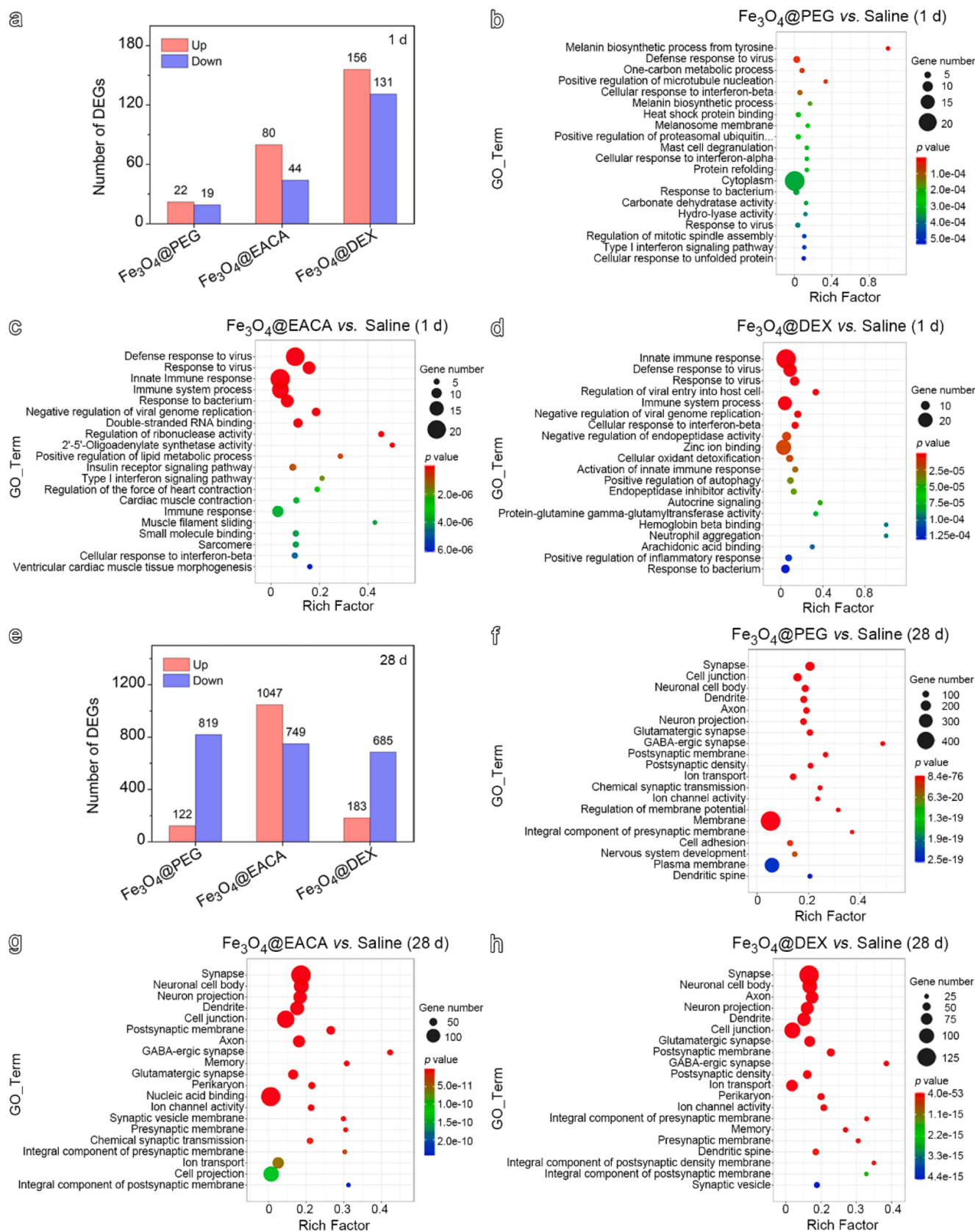


Fig. 5. Differentially expressed genes (DEGs) after exposure to Fe₃O₄@PEG, Fe₃O₄@EACA, and Fe₃O₄@DEX compared to the saline. (a) Number of DEGs between each Fe₃O₄ nanoparticles and control groups on day 1. (b-d) Bubble chart showing GO enrichment analysis of DEGs between each Fe₃O₄ nanoparticles and control groups on day 1. Y-axis and X-axis show the top 20 GO pathways and the percentages of DEGs in each pathway, respectively. The size and color of bubbles indicate the number of DEGs and *p* value ranges, respectively. (e) Number of DEGs between each Fe₃O₄ nanoparticles and control groups on day 28. (f-h) Bubble charts showing GO enrichment analysis of DEGs between each Fe₃O₄ nanoparticles and control groups on day 28.

synapse, cell junction, neuronal cell body, dendrite, and axon) and ion transport processes (e.g., ion transport and ion channel activity) are presented in all groups. Moreover, as shown in Fig. S13, these DEGs were mainly enriched in signal transduction pathways, including nicotine addiction, neuroactive ligand-receptor interaction, pancreatic secretion, synaptic vesicle cycle, retrograde endocannabinoid signaling pathways, etc.

Changes of metabolites in mouse spleen

Considering the abundant metabolic processes of DEGs observed in the Fe₃O₄ nanoparticles groups, metabolomic analysis was conducted to explore the alterations in spleen metabolic profiles upon exposure to Fe₃O₄ nanoparticles. Fig. S14 showed the univariate statistical analysis of significantly differential metabolites (DMs) in the spleen between Fe₃O₄ nanoparticles groups and the control group 1 d postinjection. As shown in Fig. 6a, only 7 DMs are found down-regulated in the Fe₃O₄@PEG group. In contrast, in the Fe₃O₄@EACA group, 20 DMs are upregulated and 8 DMs are downregulated, and in the Fe₃O₄@DEX group, 17 DMs are upregulated and 25 DMs are downregulated. Obviously, Fe₃O₄@PEG induces the smallest changes in the number of DMs, which is consistent with the results of DEGs. With respect to Fe₃O₄@EACA and Fe₃O₄@DEX groups, the qualitative analysis of differential metabolite types in Fig. 6b reveals that the majority of changes occur in lipids and lipids-like molecules, accounting for 21.4 % (Fe₃O₄@EACA) and 35.7 % (Fe₃O₄@DEX) of the total DMs.

After screening the significant DMs, KEGG pathway analysis was also performed to identify the perturbed biological pathways. As there were too few DMs in the Fe₃O₄@PEG group for conducting the metabolite pathway analysis, the hierarchical clustering of DMs was focused on the Fe₃O₄@EACA and Fe₃O₄@DEX groups. As shown in Fig. 6c, d, a total of 8 and 12 related pathways are identified for Fe₃O₄@EACA group and Fe₃O₄@DEX group, respectively. Importantly, the DMs are mostly enriched in the cholesterol, fat, lipid, steroid, and choline metabolism pathways. These results suggest that Fe₃O₄@EACA and Fe₃O₄@DEX perturb spleen metabolism mainly through the disruption of lipid metabolism, while Fe₃O₄@PEG appears to have a minimal impact on the spleen metabolism.

DMs analysis was also performed to disclose the long-term effects on metabolites, 28 d after the intravenous injection of the nanoparticles (Fig. S15). As shown in Fig. 6e, a greater number of spleen metabolites undergo significant changes. In detail, there are 50 DMs upregulated and 9 DMs downregulated for Fe₃O₄@PEG group, 23 DMs upregulated and 6 DMs downregulated for Fe₃O₄@EACA group, and 49 DMs upregulated and 34 DMs downregulated for Fe₃O₄@DEX group. Moreover, the results in Fig. S16 indicated that the majority of DMs induced by Fe₃O₄@PEG, Fe₃O₄@EACA, and Fe₃O₄@DEX were mainly lipids and lipids-like molecules over long-term.

The KEGG pathway enrichment analyses in Fig. 6f-h reveal that the DMs of Fe₃O₄@PEG, Fe₃O₄@EACA, and Fe₃O₄@DEX groups are significantly enriched in different pathways. As shown in Fig. 6f, the significantly DMs induced by Fe₃O₄@PEG are mostly enriched in apoptosis and necroptosis pathways. Additionally, choline metabolism in the spleen cells is changed significantly, along with lipids, e.g., sphingolipid, ether lipid, sphingolipid, and glycerophospholipid. Simultaneous changes in glutathione metabolism, ferroptosis, and chemical carcinogenesis-ROS pathways are observed in the Fe₃O₄@EACA group, as shown in Fig. 6g, indicating the upregulated glutathione metabolism for balancing the enhanced oxidative stress caused by iron ions released by Fe₃O₄@EACA [46]. With respect to Fe₃O₄@DEX group, Fig. 6h reveals that DMs are primarily enriched in signal transduction pathways, including Fc gamma R-mediated phagocytosis, apelin signaling, phospholipase D signaling, calcium signaling, and sphingolipid signaling pathways. Furthermore, DMs related to amino acids metabolism and lipids metabolism are also observed in the Fe₃O₄@DEX group.

Biosafety evaluation

In order to assess the biosafety of Fe₃O₄ nanoparticles, a series of toxicological evaluations were conducted. The body weights of mice exposed to three types of Fe₃O₄ nanoparticles and saline, respectively, were monitored over a 28-day period. As shown in Fig. S17a, no significant differences in the body weights were observed between the Fe₃O₄ nanoparticles groups and saline group. The organ index results in Fig. S17b showed no significant changes in major organs (i.e., heart, liver, spleen, lung, kidney, and brain) of the three Fe₃O₄ nanoparticles groups, even in organs like the liver and spleen where Fe₃O₄ nanoparticles tend to be accumulated. Additionally, negligible liver toxicities were observed from all groups through the levels of alanine aminotransferase (ALT), aspartate aminotransferase (AST), alkaline phosphatase (ALP) and gamma glutamyl transferase (GGT), as demonstrated in Fig. S18a-d. Similarly, there was no significant kidney toxicity in all groups observed through the analysis on creatinine (CREA) and blood urea (UREA) levels (Fig. S18e, f). Furthermore, as shown in Fig. S19, obvious differences in peripheral circulating blood cell counts were not observed following systemic exposure to the three kinds of Fe₃O₄ nanoparticles. All alterations in clinical chemistry parameters and hematological parameters, including those that exhibit statistically significant differences, are not considered indicative of toxicity induced by the three Fe₃O₄ nanoparticles, as these changes could be ignored in magnitude, specifically could be considered within the normal range of biological variation or without toxicological significance. Finally, histopathological examinations of tissues from both saline and Fe₃O₄ nanoparticles groups were performed. The results of hematoxylin-eosin (H&E) staining in Fig. S20 showed that none of the three Fe₃O₄ nanoparticles induced any observable inflammation, pathological abnormalities, or histopathological tissue damage in the main organs of mice.

Discussion

Putting all the above results together, we attempt to reveal how surface chemistry-related protein corona disturbs the immune responses of Fe₃O₄ nanoparticles in the spleen. After intravenous administration, three types of Fe₃O₄ nanoparticles are rapidly covered by various plasma proteins to form unique opsonins-rich protein coronas, including immunoglobulins, coagulations, and complements, e.g., IGHM, PF4, THBS1, C1QB, C3, and MBL1, which play a key role in the immune responses of the host. Previous studies have shown that nanomaterials bound to opsonins can significantly enhance the production and release of proinflammatory cytokines and upregulate the levels of immune cells [18,41,47]. In addition, selective adsorption of complement recognition molecules on nanomaterials can also activate the complement system [48,49]. As seen before, among the three types of Fe₃O₄ nanoparticles, Fe₃O₄@PEG exhibits the smallest level of proteins adsorption due to its weak negative charge and excellent hydrophilicity, which reduce its electrostatic and hydrophobic interactions with proteins [40,50,51]. Meanwhile, more abundant opsonins are found on the surface of Fe₃O₄@EACA and Fe₃O₄@DEX than Fe₃O₄@PEG, which helps us speculate that these nanoparticles may induce stronger immunological effects in the spleen.

After entering the spleen, Fe₃O₄ nanoparticles inevitably interact with immune cells in the spleen and subsequently trigger a series of responses. As expected, diverse cells populations, gene expression, and metabolites in the spleen are particularly sensitive within a short period, e.g., 1 d. It's observed that all Fe₃O₄ nanoparticles affect proliferation of different innate immune cells, indicating that they may all trigger innate immune responses in the spleen. Subsequently, DEGs results show that the Fe₃O₄@PEG group displays the smallest number of DEGs compared to the Fe₃O₄@EACA and Fe₃O₄@DEX groups. Meanwhile, in the Fe₃O₄@EACA and Fe₃O₄@DEX groups, GO enrichment analysis reveals a large number of DEGs related to immune response pathways, obviously indicating that they elicit stronger immune responses than the

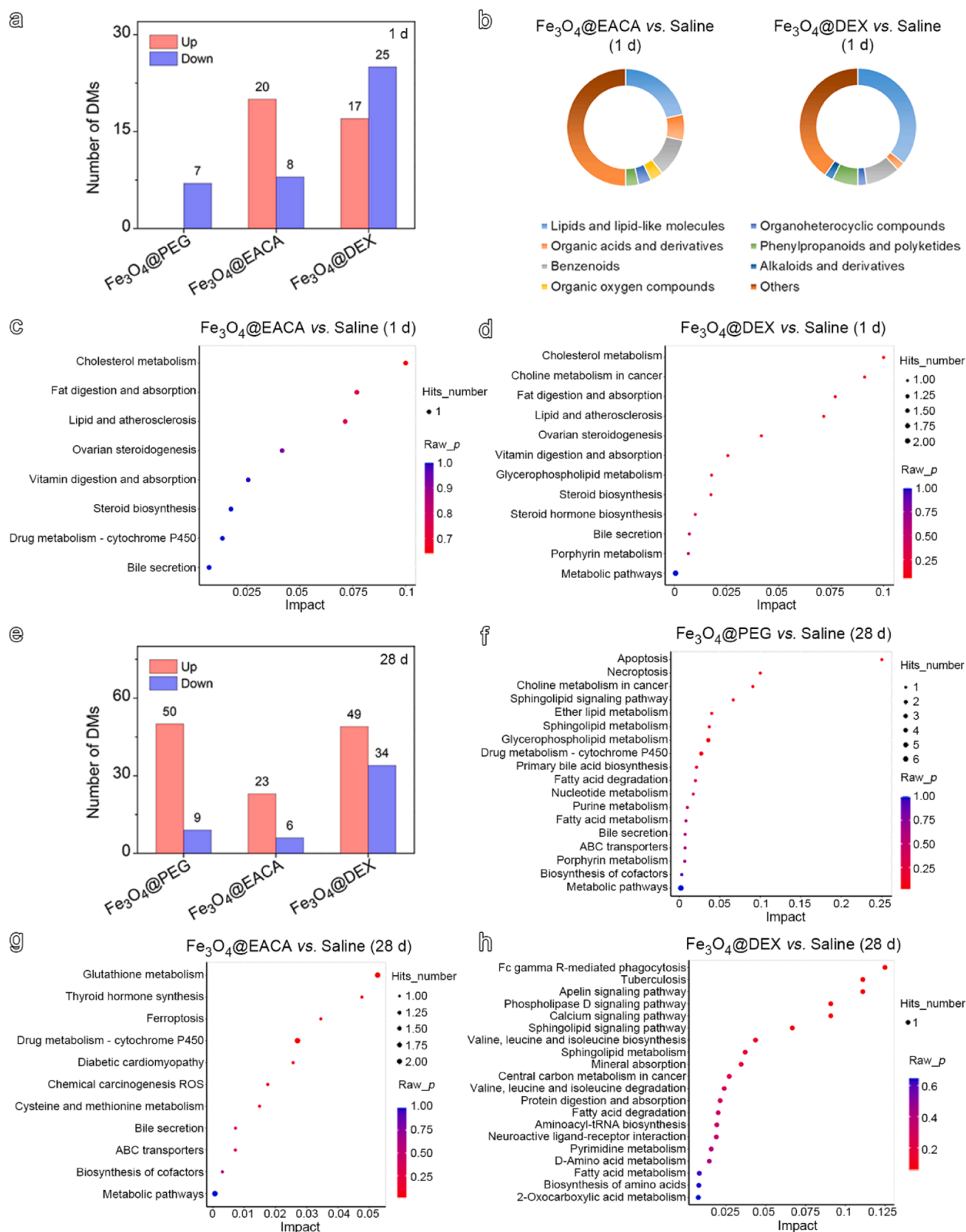


Fig. 6. Differential metabolites (DMs) after exposure to Fe₃O₄@PEG, Fe₃O₄@EACA, and Fe₃O₄@DEX compared to saline. (a) Number of DMs between each Fe₃O₄ nanoparticles and control groups on day 1. (b) Relative abundance of DMs categories between Fe₃O₄ nanoparticles and control groups on day 1. (c-d) KEGG pathway enrichment analysis for Fe₃O₄@EACA group and Fe₃O₄@DEX group on day 1. Y-axis and X-axis show KEGG pathways and the percentages of DMs in each pathway, respectively. The size and color of bubbles indicate the number of DMs and raw *p* value ranges, respectively. (e) Number of DMs between each Fe₃O₄ nanoparticles and control groups on day 28. (f-h) KEGG pathway enrichment analysis for the Fe₃O₄@PEG, Fe₃O₄@EACA, and Fe₃O₄@DEX groups on day 28.

Fe₃O₄@PEG group, which is consistent with the result regarding the lowest absorption of opsonins by Fe₃O₄@PEG. KEGG enrichment analysis demonstrates that complement and coagulation cascades pathway is the most relevant pathway of DEGs in Fe₃O₄@DEX group, implying that the complement system may be activated, which may be attributed to the high enrichment of complement system related proteins, *i.e.*, C3, PF4, MBL1, and *etc.* [42,43,52] This result could explain why Fe₃O₄@DEX induces disturbances in the spleen similar to those caused by Fe₃O₄@EACA, despite the former adsorbs fewer proteins than the latter. With respect to metabolism, the minimum numbers of DMs also occur in the Fe₃O₄@PEG group. Moreover, cholesterol, fat, and lipid metabolisms are rapidly affected in the Fe₃O₄@EACA and Fe₃O₄@DEX groups, which may be related to the immune response of these nanoparticles in the spleen. Chen et al. have reported that the dynamic intracellular exchange of protein corona on the nanomaterials will disrupt proteostasis and the key cellular metabolism pathway, including glycolysis and lipid metabolism [53]. Therefore, it seems reasonable to assume that the opsonins absorbed on Fe₃O₄@EACA and Fe₃O₄@DEX may exchange with other biomolecules inside and outside immune cells, then greatly alter the metabolisms in the spleen. Based on the above results, it can be concluded that such abundant opsonins in the protein corona of Fe₃O₄ nanoparticles can significantly enhance subsequent immune responses in the spleen. It can further be concluded that the surface chemistry of nanoparticles plays a critical role in activating the immune responses of the host because it is closely related to the protein composition of the corona.

As time goes on, the Fe₃O₄ nanoparticles in the spleen gradually undergo degradation [54,55]. Notably, compared to the results determined 1 d postinjection, the levels of immune cells, DEGs, and DMs were enhanced over 28 d postinjection, which is possibly due to the influence of iron ions released from Fe₃O₄ nanoparticles. It has been reported that iron element plays an important role in cell proliferation [56–58]. Therefore, the enhanced levels of macrophages, DCs, and B cells may be caused by iron ions rather than Fe₃O₄ nanoparticles themselves. From further DEGs analysis, no pathways related to immune response is observed, but the pathways associated with intercellular interactions and ion transport are evident. The enrichment of DMs on the cell death and ferroptosis pathways also prove the effect of iron ions on the spleen. Furthermore, the long-term biosafety assessment demonstrates that intravenously delivered Fe₃O₄ nanoparticles don't cause obvious toxicity, indicating that the iron ions slowly released by Fe₃O₄ nanoparticles do not trigger enough ferroptosis to damage the spleen obviously.

Conclusion

This study aimed to disclose the biological effects of Fe₃O₄ nanoparticles on the spleen by focusing on protein corona that was tuned through well-established surface chemistry, with the objective of assessing their potential clinical benefits. Our findings reveal that the diphosphonate- ϵ -aminocaproic acid- and carboxymethyl dextran-coated Fe₃O₄ nanoparticles induce a higher degree of immune responses in the spleen compared to PEG-coated Fe₃O₄ counterparts, owing to the enriched opsonins on the particle surfaces. These responses are manifested by changes in immune cells proliferation, gene expression, and metabolites profiles, underscoring the pivotal role of protein corona in the immune responses elicited by nanomaterials in the spleen. Under the clinical injection dosage of Fe₃O₄ nanoparticle for MRI applications, PEG coating presents an outstanding safety profile, making it potentially suitable for future clinical use. In contrast, opsonins-rich protein corona on Fe₃O₄ nanoparticles coated with diphosphonate- ϵ -aminocaproic acid- or carboxymethyl dextran triggers stronger immune responses in the spleen, which may raise safety concerns. Different from the situations in the liver, the recognition and response of nanoparticles in the spleen are more reflected by systemic immune regulation which is largely taken as a major origin of the safety risks for nanoparticles [6,59,

60]. In this respect, the current studies focusing on the immune responses elicited by nanoparticles in the spleen may provide valuable fundamental information on the immune responses of nanoparticles, superficially associated with the protein corona, but intrinsically associated with the surface chemistry of nanoparticles.

CRedit authorship contribution statement

Can Chen: Data curation, Writing – original draft, Visualization, Investigation. **Yueping Li:** Visualization, Investigation. **Dandan Zhou:** Visualization, Investigation. **Jiada Fan:** Visualization, Investigation. **Xuelan Hu:** Visualization, Investigation. **Ruru Zhang:** Visualization, Investigation. **Jianxian Ge:** Visualization, Investigation. **Xiaoyi Cao:** Visualization, Investigation. **Haodi Qi:** Visualization, Investigation. **Ning Wang:** Visualization, Investigation. **Lei Chen:** Visualization, Investigation. **Baoxing Huang:** Visualization, Investigation. **Jianfeng Zeng:** Conceptualization, Funding acquisition, Methodology, Supervision, Writing – review & editing. **Mingyuan Gao:** Conceptualization, Funding acquisition, Methodology, Supervision, Writing – review & editing.

Declaration of Competing Interest

The authors declare that they have no known competing financial interests or personal relationships that could have appeared to influence the work reported in this paper.

Acknowledgements

The authors thank the financial support from National Natural Science Foundation of China (82130059, 82222033, 82172003), National Key Research and Development Program of China (2018YFA0208800), and Priority Academic Program Development of Jiangsu Higher Education Institutions (PAPD).

Appendix A. Supporting information

Supplementary data associated with this article can be found in the online version at [doi:10.1016/j.nantod.2025.102676](https://doi.org/10.1016/j.nantod.2025.102676).

Data availability

No data was used for the research described in the article.

References

- [1] J. Liu, M. Guo, C. Chen, Nano-bio interactions: a major principle in the dynamic biological processes of nano-assemblies, *Adv. Drug. Deliv. Rev.* 186 (2022) 114318.
- [2] X. Wang, X. Zhong, J. Li, Z. Liu, L. Cheng, Inorganic nanomaterials with rapid clearance for biomedical applications, *Chem. Soc. Rev.* 50 (15) (2021) 8669–8742.
- [3] W. Ngo, S. Ahmed, C. Blackadar, B. Bussin, Q. Ji, S.M. Mladjenovic, Z. Sepahi, W.C. W. Chan, Why nanoparticles prefer liver macrophage cell uptake *in vivo*, *Adv. Drug Deliv. Rev.* 185 (2022) 114238.
- [4] M. Cao, R. Cai, L. Zhao, M. Guo, L. Wang, Y. Wang, L. Zhang, X. Wang, H. Yao, C. Xie, Y. Cong, Y. Guan, X. Tao, Y. Wang, S. Xu, Y. Liu, Y. Zhao, C. Chen, Molybdenum derived from nanomaterials incorporates into molybdenum enzymes and affects their activities *in vivo*, *Nat. Nanotechnol.* 16 (2021) 708–716.
- [5] L. Newman, D.A. Jasim, E. Prestat, N. Lozano, I. de Lazaro, Y. Nam, B.M. Assas, J. Pennock, S.J. Haigh, C. Bussy, K. Kostarelou, Splenic capture and *in vivo* intracellular biodegradation of biological-grade graphene oxide sheets, *ACS Nano* 14 (8) (2020) 10168–10186.
- [6] S.M. Lewis, A. Williams, S.C. Eisenbarth, Structure and function of the immune system in the spleen, *Sci. Immunol.* 4 (2019) 6085.
- [7] T. Zhang, T. Lei, R. Yan, B. Zhou, C. Fan, Y. Zhao, S. Yao, H. Pan, Y. Chen, B. Wu, Y. Yang, L. Hu, S. Gu, X. Chen, F. Bao, Y. Li, H. Xie, R. Tang, X. Chen, Z. Yin, Systemic and single cell level responses to 1 nm size biomaterials demonstrate distinct biological effects revealed by multi-omics atlas, *Bioact. Mater.* 18 (2022) 199–212.
- [8] J. Chen, S. Zhang, J. Tong, X. Teng, Z. Zhang, S. Li, X. Teng, Whole transcriptome-based miRNA-mRNA network analysis revealed the mechanism of inflammation-

- immunosuppressive damage caused by cadmium in common carp spleens, *Sci. Total Environ.* 717 (2020) 137081.
- [9] J. Szebeni, G. Storm, J.Y. Ljubimova, M. Castells, E.J. Phillips, K. Turjeman, Y. Barenholz, D.J.A. Crommelin, M.A. Dobrovolskaia, Applying lessons learned from nanomedicines to understand rare hypersensitivity reactions to mRNA-based SARS-CoV-2 vaccines, *Nat. Nanotechnol.* 17 (4) (2022) 337–346.
- [10] J. Szebeni, Mechanism of nanoparticle-induced hypersensitivity in pigs: complement or not complement? *Drug Discov. Today* 23 (3) (2018) 487–492.
- [11] N. Luo, J.K. Weber, S. Wang, B. Luan, H. Yue, X. Xi, J. Du, Z. Yang, W. Wei, R. Zhou, G. Ma, PEGylated graphene oxide elicits strong immunological responses despite surface passivation, *Nat. Commun.* 8 (2017) 14537.
- [12] S.M. Jin, Y.J. Yoo, H.S. Shin, S. Kim, S.N. Lee, C.H. Lee, H. Kim, J.E. Kim, Y.S. Bae, J. Hong, Y.W. Noh, Y.T. Lim, A nanoadjuvant that dynamically coordinates innate immune stimuli activation enhances cancer immunotherapy and reduces immune cell exhaustion, *Nat. Nanotechnol.* 18 (4) (2023) 390–402.
- [13] J.L. Liang, X.K. Jin, G.F. Luo, S.M. Zhang, Q.X. Huang, Y.T. Lin, X.C. Deng, J. W. Wang, W.H. Chen, X.Z. Zhang, Immunostimulant hydrogel-guided tumor microenvironment reprogramming to efficiently potentiate macrophage-mediated cellular phagocytosis for systemic cancer immunotherapy, *ACS Nano* 17 (17) (2023) 17217–17232.
- [14] J. Ren, N. Andrikopoulos, K. Velonia, H. Tang, R. Cai, F. Ding, P.C. Ke, C. Chen, Chemical and biophysical signatures of the protein corona in nanomedicine, *J. Am. Chem. Soc.* 144 (21) (2022) 9184–9205.
- [15] K.E. Wheeler, A.J. Chetwynd, K.M. Fahy, B.S. Hong, J.A. Tochiwilt, L.A. Foster, I. Lynch, Environmental dimensions of the protein corona, *Nat. Nanotechnol.* 16 (6) (2021) 617–629.
- [16] M. Li, X. Jin, T. Liu, F. Fan, F. Gao, S. Chai, L. Yang, Nanoparticle elasticity affects systemic circulation lifetime by modulating adsorption of apolipoprotein A-I in corona formation, *Nat. Commun.* 13 (1) (2022) 4137.
- [17] H. Tang, Y. Zhang, T. Yang, C. Wang, Y. Zhu, L. Qiu, J. Liu, Y. Song, L. Zhou, J. Zhang, Y.K. Wong, Y. Liu, C. Xu, H. Wang, J. Wang, Cholesterol modulates the physiological response to nanoparticles by changing the composition of protein Corona, *Nat. Nanotechnol.* 18 (9) (2023) 1067–1077.
- [18] J.Y. Park, S.J. Park, J.Y. Park, S.H. Kim, S. Kwon, Y. Jung, D. Khang, Unfolded protein corona surrounding nanotubes influence the innate and adaptive immune system, *Adv. Sci.* 8 (8) (2021) 2004979.
- [19] R. Qiao, C. Fu, H. Forgham, I. Javed, X. Huang, J. Zhu, A.K. Whittaker, T.P. Davis, Magnetic iron oxide nanoparticles for brain imaging and drug delivery, *Adv. Drug Deliv. Rev.* 197 (2023) 114822.
- [20] S.A. Sankaranarayanan, A. Thomas, N. Revi, B. Ramakrishna, A.K. Rengan, Iron oxide nanoparticles for theranostic applications—recent advances, *J. Drug Deliv. Sci. Technol.* 70 (2022) 103196.
- [21] H. Etemadi, J.K. Buchanan, N.G. Kandile, P.G. Plieger, Iron oxide nanoparticles: Physicochemical characteristics and historical developments to commercialization for potential technological applications, *ACS Biomater. Sci. Eng.* 7 (12) (2021) 5432–5450.
- [22] Q. Liu, J. Zou, Z. Chen, W. He, W. Wu, Current research trends of nanomedicines, *Acta Pharm. Sin.* B 13 (11) (2023) 4391–4416.
- [23] C.G. Varallyay, G.B. Toth, R. Fu, J.P. Netto, J. Firkins, P. Ambady, E.A. Neuwelt, What does the boxed warning tell us? Safe practice of using ferumoxytol as an MRI contrast agent, *AJNR Am. J. Neuroradiol.* 38 (7) (2017) 1297–1302.
- [24] L. Chen, Y. Gao, J. Ge, Y. Zhou, Z. Yang, C. Li, B. Huang, K. Lu, D. Kou, D. Zhou, C. Chen, S. Wang, S. Wu, J. Zeng, G. Huang, M. Gao, A clinically translatable kit for MRI/NMI dual-modality nanoprobes based on anchoring group-mediated radiolabeling, *Nanoscale* 15 (8) (2023) 3991–3999.
- [25] L. Chen, J. Ge, B. Huang, D. Zhou, G. Huang, J. Zeng, M. Gao, Anchoring group mediated radiolabeling for achieving robust nanoimaging probes, *Small* 17 (51) (2021) 2104977.
- [26] C. Chen, B. Huang, R. Zhang, C. Sun, L. Chen, J. Ge, D. Zhou, Y. Li, S. Wu, Z. Qian, J. Zeng, M. Gao, Surface ligand-regulated renal clearance of MRI/SPECT dual-modality nanoprobes for tumor imaging, *J. Nanobiotechnol.* 22 (1) (2024) 245.
- [27] C. Chen, J. Ge, Y. Gao, L. Chen, J. Cui, J. Zeng, M. Gao, Ultrasmall superparamagnetic iron oxide nanoparticles: a next generation contrast agent for magnetic resonance imaging, *WIREs Nanomed. Nanobiotechnol.* 14 (1) (2021) 1740.
- [28] J. Yang, J. Feng, S. Yang, Y. Xu, Z. Shen, Exceedingly small magnetic iron oxide nanoparticles for T₁-weighted magnetic resonance imaging and imaging-guided therapy of tumors, *Small* 19 (49) (2023) 2302856.
- [29] R. Chen, D. Ling, L. Zhao, S. Wang, Y. Liu, R. Bai, S. Baik, Y. Zhao, C. Chen, T. Hyeon, Parallel comparative studies on mouse toxicity of oxide nanoparticle- and gadolinium-based T₁ MRI contrast agents, *ACS Nano* 9 (12) (2015) 12425–12435.
- [30] Q. Weng, X. Hu, J. Zheng, F. Xia, N. Wang, H. Liao, Y. Liu, D. Kim, J. Liu, F. Li, Q. He, B. Yang, C. Chen, T. Hyeon, D. Ling, Toxicological risk assessments of iron oxide nanocluster- and gadolinium-based T₁ MRI contrast agents in renal failure rats, *ACS Nano* 13 (6) (2019) 6801–6812.
- [31] J. Zeng, L. Jing, Y. Hou, M. Jiao, R. Qiao, Q. Jia, C. Liu, F. Fang, H. Lei, M. Gao, Anchoring group effects of surface ligands on magnetic properties of Fe₃O₄ nanoparticles: towards high performance MRI contrast agents, *Adv. Mater.* 26 (17) (2014) 2694–2698.
- [32] A. Dong, X. Ye, J. Chen, Y. Kang, T. Gordon, J.M. Kikkawa, C.B. Murray, A generalized ligand-exchange strategy enabling sequential surface functionalization of colloidal nanocrystals, *J. Am. Chem. Soc.* 133 (4) (2011) 998–1006.
- [33] Z. Wang, Q. Ye, S. Yu, B. Akhavan, Poly ethylene glycol (PEG)-based hydrogels for drug delivery in cancer therapy: a comprehensive review, *Adv. Healthc. Mater.* 12 (18) (2023) 2300105.
- [34] A.A. D'souza, R. Shegokar, Polyethylene glycol (PEG): a versatile polymer for pharmaceutical applications, *Expert Opin. Drug Del.* 13 (9) (2016) 1257–1275.
- [35] I.C. Macdougall, W.E. Strauss, J. McLaughlin, Z. Li, F. Dellanna, J. Hertel, A randomized comparison of ferumoxytol and iron sucrose for treating iron deficiency anemia in patients with CKD, *Clin. J. Am. Soc. Nephro.* 9 (4) (2014) 705–712.
- [36] J. Ge, L. Chen, B. Huang, Y. Gao, D. Zhou, Y. Zhou, C. Chen, L. Wen, Q. Li, J. Zeng, Z. Zhong, M. Gao, Anchoring group-mediated radiolabeling of inorganic nanoparticles—a universal method for constructing nuclear medicine imaging nanoprobes, *ACS Appl. Mater. Interfaces* 14 (7) (2022) 8838–8846.
- [37] F. Guo, S. Luo, L. Wang, M. Wang, F. Wu, Y. Wang, Y. Jiao, Y. Du, Q. Yang, X. Yang, G. Yang, Protein corona, influence on drug delivery system and its improvement strategy: a review, *Int. J. Biol. Macromol.* 256 (2024) 128513.
- [38] X. Wang, W. Zhang, The Janus of protein corona on nanoparticles for tumor targeting, immunotherapy and diagnosis, *J. Control. Release* 345 (2022) 832–850.
- [39] M.J. Hajipour, R. Safavi-Sohi, S. Sharifi, N. Mahmoud, A.A. Ashkarran, E. Voke, V. Serpooshan, M. Ramezankhani, A.S. Milani, M.P. Landry, M. Mahmoudi, An overview of nanoparticle protein corona literature, *Small* 19 (36) (2023) e2301838.
- [40] M. Martinez-Negro, G. Gonzalez-Rubio, E. Aicart, K. Landfester, A. Guerrero-Martinez, E. Junquera, Insights into colloidal nanoparticle-protein corona interactions for nanomedicine applications, *Adv. Colloid Interface Sci.* 289 (2021) 102366.
- [41] J. Mo, Q. Xie, W. Wei, J. Zhao, Revealing the immune perturbation of black phosphorus nanomaterials to macrophages by understanding the protein corona, *Nat. Commun.* 9 (1) (2018) 2480.
- [42] S. Khandelwal, J.M. Alexandra, C.G. Hester, M.M. Frank, G.M. Arepally, Mechanism of complement activation by PF4/Heparin complexes, *Blood* 128 (22) (2016), 137–137.
- [43] E. Hertle, M.M. van Greevenbroek, C.D. Stehouwer, Complement C3: an emerging risk factor in cardiometabolic disease, *Diabetologia* 55 (4) (2012) 881–884.
- [44] S. Tenzer, D. Docter, J. Kuharev, A. Musyanovych, V. Fetz, R. Hecht, F. Schlenk, D. Fischer, K. Kiouptsi, C. Reinhardt, K. Landfester, H. Schild, M. Maskos, S. K. Knauer, R.H. Stauber, Rapid formation of plasma protein corona critically affects nanoparticle pathophysiology, *Nat. Nanotechnol.* 8 (10) (2013) 772–781.
- [45] K.H. Park, K. Kurokawa, L. Zheng, D.J. Jung, K. Tateishi, J.O. Jin, N.C. Ha, H. J. Kang, M. Matsushita, J.Y. Kwak, K. Takahashi, B.L. Lee, Human serum mannose-binding lectin senses wall teichoic acid glycopolymer of staphylococcus aureus, which is restricted in infancy, *J. Biol. Chem.* 285 (35) (2010) 27167–27175.
- [46] A. Tarangel, J. Rodencal, J.T. Kim, L. Magtanong, J.Z. Long, S.J. Dixon, Nucleotide biosynthesis links glutathione metabolism to ferroptosis sensitivity, *Life Sci. Alliance* 5 (4) (2022) e202101157.
- [47] L. Digiaco, D. Pozzi, S. Palchetti, A. Zingoni, G. Caracciolo, Impact of the protein corona on nanomaterial immune response and targeting ability, *WIREs Nanomed. Nanobiotechnol.* 12 (4) (2020) e1615.
- [48] V.P. Vu, G.B. Gifford, F. Chen, H. Benasutti, G. Wang, E.V. Groman, R. Scheinman, L. Saba, S.M. Moghimi, D. Simberg, Immunoglobulin deposition on biomolecule corona determines complement opsonization efficiency of preclinical and clinical nanoparticles, *Nat. Nanotechnol.* 14 (3) (2019) 260–268.
- [49] F. Chen, G. Wang, J.L. Griffin, B. Breneman, N.K. Banda, V.M. Holers, D.S. Backos, L. Wu, S.M. Moghimi, D. Simberg, Complement proteins bind to nanoparticle protein corona and undergo dynamic exchange *in vivo*, *Nat. Nanotechnol.* 12 (4) (2017) 387–393.
- [50] K. Saha, M. Rahimi, M. Yazdani, S.T. Kim, D.F. Moyano, S. Hou, R. Das, R. Mout, F. Rezaee, M. Mahmoudi, V.M. Rotello, Regulation of macrophage recognition through the interplay of nanoparticle surface functionality and protein corona, *ACS Nano* 10 (4) (2016) 4421–4430.
- [51] R. Cai, J. Ren, Y. Ji, Y. Wang, Y. Liu, Z. Chen, Z. Farhadi Sabet, X. Wu, I. Lynch, C. Chen, Corona of thorns: The surface chemistry-mediated protein corona perturbs the recognition and immune response of macrophages, *ACS Appl. Mater. Interfaces* 12 (2) (2020) 1997–2008.
- [52] L. Neglia, M. Oggioni, D. Mercurio, M.G. De Simoni, S. Fumagalli, Specific contribution of mannose-binding lectin murine isoforms to brain ischemia/reperfusion injury, *Cell. Mol. Immunol.* 17 (3) (2020) 218–226.
- [53] R. Cai, J. Ren, M. Guo, T. Wei, Y. Liu, C. Xie, P. Zhang, Z. Guo, A.J. Chetwynd, P. C. Ke, I. Lynch, C. Chen, Dynamic intracellular exchange of nanomaterials' protein corona perturbs proteostasis and remodels cell metabolism, *Proc. Natl. Acad. Sci. U. S. A.* 119 (23) (2022) e2200363119.
- [54] J. Volatrou, F. Carn, J. Kolosnjaj-Tabi, Y. Javed, Q.L. Vuong, Y. Gossuin, C. Menager, N. Luciani, G. Charron, M. Hemadi, D. Alloyeau, F. Gazeau, Ferritin protein regulates the degradation of iron oxide nanoparticles, *Small* 13 (2) (2017) 1602030.
- [55] Z. Yang, S. Wu, Y. Gao, D. Kou, K. Lu, C. Chen, Y. Zhou, D. Zhou, L. Chen, J. Ge, C. Li, J. Zeng, M. Gao, Unveiling the biologically dynamic degradation of iron oxide nanoparticles via a continuous flow system, *Small Methods* 8 (3) (2024) e2301479.
- [56] Y. Jiang, C. Li, Q. Wu, P. An, L. Huang, J. Wang, C. Chen, X. Chen, F. Zhang, L. Ma, S. Liu, H. He, S. Xie, Y. Sun, H. Liu, Y. Zhan, Y. Tao, Z. Liu, X. Sun, Y. Hu, Q. Wang, D. Ye, J. Zhang, S. Zou, Y. Wang, G. Wei, Y. Liu, Y. Shi, Y. Eugene Chin, Y. Hao, F. Wang, X. Zhang, Iron-dependent histone 3 lysine 9 demethylation controls B cell proliferation and humoral immune responses, *Nat. Commun.* 10 (1) (2019) 2935.
- [57] R.A. Weber, F.S. Yen, S.P.V. Nicholson, H. Alwaseem, E.C. Bayraktar, M. Alam, R. C. Timson, K. La, M. Abu-Remaileh, H. Molina, K. Birsoy, Maintaining iron

- homeostasis is the key role of lysosomal acidity for cell proliferation, *Mol. Cell* 77 (3) (2020) 645–655.
- [58] E. Abboud, D. Chrayteh, N. Boussetta, H. Dalle, M. Malerba, T.D. Wu, M. Le Gall, O. Reelfs, C. Pourzand, M. Mellet, F. Assan, H. Bachelez, J. Poupon, S. Aractingi, S. Vaulont, P. Sohier, B. Oules, Z. Karim, C. Peyssonnaud, Skin hepcidin initiates psoriasisform skin inflammation via Fe-driven hyperproliferation and neutrophil recruitment, *Nat. Commun.* 15 (1) (2024) 6718.
- [59] P. Kubers, C. Jenne, Immune responses in the liver, *Annu. Rev. Immunol.* 36 (2018) 247–277.
- [60] V. Bronte, Mikael J. Pittet, The spleen in local and systemic regulation of immunity, *Immunity* 39 (5) (2013) 806–818.